Advanced Composite Materials
Publication details, including instructions for authors and subscription information:
http://www.tandfonline.com/loi/tacm20

Strain monitoring of braided composites by using embedded fiber-optic strain sensors

Tatsuro Kosaka , Hideaki Kurimoto , Katsuhiko Osaka , Asami Nakai , Toshiko Osada , Hiroyuki Hamada & Takehito Fukuda

Version of record first published: 02 Apr 2012.

To cite this article: Tatsuro Kosaka , Hideaki Kurimoto , Katsuhiko Osaka , Asami Nakai , Toshiko Osada , Hiroyuki Hamada & Takehito Fukuda (2004): Strain monitoring of braided composites by using embedded fiber-optic strain sensors, Advanced Composite Materials, 13:3-4, 157-170

To link to this article: http://dx.doi.org/10.1163/1568551042580172

Adv. Composite Mater., Vol. 13, No. 3-4, pp. 157–170 (2004)

Also available online - www.vsppub.com

Strain monitoring of braided composites by using embedded fiber-optic strain sensors

TATSURO KOSAKA [1,*], HIDEAKI KURIMOTO [1], KATSUHIKO OSAKA [1], ASAMI NAKAI [2], TOSHIKO OSADA [2], HIROYUKI HAMADA [2] and TAKEHITO FUKUDA [3]

[1] *Graduate School of Engineering, Osaka City University, Department of Intelligent Materials Engineering, Sugimoto 3, Sumiyoshi, Osaka 558-8585, Japan*
[2] *Division of Advanced Fibro-Science, Graduate School, Kyoto Institute of Technology, Matugasaki, Sakyo-ku, Kyoto 606-8585, Japan*
[3] *Collaborative Research Center for Industry Creation, Osaka City University, Sugimoto 3, Sumiyoshi, Osaka 558-8585, Japan*

Received 16 May 2002; accepted 28 May 2004

Abstract—Recently, fiber optic strain sensors have been applied to internal strain and damage monitoring of composites because of their small size, light weight and flexibility. Braided fiber reinforced plastics (FRP) are compatible with fiber optic sensors because optical fibers can be integrated directly and easily into fabrics. In the present paper, the strain monitoring of braided glass fiber reinforced plastics (GFRP) was conducted by using embedded fiber Bragg grating (FBG) and extrinsic Fabry–Perot interferometric (EFPI) sensors during the cure process, tensile tests and fatigue tests. From the experimental results of cure monitoring, it was found that both sensors can be used only for monitoring of thermal residual strain during cooling process. From the results of tensile tests, it was found that both sensors could measure strain correctly until damage initiation of braided GFRP. It also appeared that FBG sensors could monitor damage to FRP by observing the reflected spectral shape. From the fatigue tests, it appeared that the strain measured by embedded FBG sensors was affected by fatigue damage. Therefore, it is concluded that internal strain monitoring of braided FRP using fiber optic strain sensors is very useful for cure and health monitoring.

Keywords: Fiber optic sensors; EFPI; FBG; braided composites; cure and health monitoring; strain monitoring; damage detection.

1. INTRODUCTION

In situ cure and health monitoring of fiber reinforced plastics (FRPs) is a very attractive technique to manufacturers and users because quality of the products

*To whom correspondence should be addressed. E-mail: kosaka@imat.eng.osaka-cu.ac.jp.

can be ensured in real time. In cure monitoring, the internal state of the FRP such as degree of cure, pressure, temperature, voids, defects and residual stress can be monitored. Such internal information of FRP is available for optimization of the curing process to reduce time of the curing cycle and enhance the quality. In addition, the quality of the product can be assessed during the cure process, which simplifies the procedure. On the other hand, a health monitoring system using integrated sensors provides self-monitoring functions of stress, strain and damage of materials. Since this monitoring system works in operation, the quality of the composite structures can always be ensured. So this technique allows us to use easy and simple periodical inspections. Several kinds of micro sensors, such as fiber optic sensors, dielectric sensors, piezoelectric sensors, etc. have been investigated as *in situ* sensors for cure and health monitoring [1].

Among *in situ* sensors, fiber-optic sensors are promising because of their small size, light weight, high strength and high flexibility. Spectroscopy-based sensors such as near-infrared spectroscopy (NIRS)-based and fluorimetry-based sensors can monitor changes in chemical construction of resin [2–4]. Refractive index-based sensors can be utilized for measurement of reflection rate between optical fibers and resin [3, 5]. Since these sensors are not so useful for health monitoring of FRP, we have considered that fiber-optic strain sensors, which can be used for both cure and health monitoring, are more useful.

Popular fiber-optic strain sensors are interferometric sensors, extrinsic Fabry–Perot interferometer (EFPI) sensors, fiber Bragg grating (FBG) sensors, and Brillouin optical time domain reflectometric (B-OTDR) sensors. Michelson interferometric sensors need two or three optical fibers, including reference fibers. Since it is difficult to embed the sensor in the FRP, it is not suitable for cure monitoring. High-speed strain measurements of FRP laminates by using Michelson interferometric sensors were reported [6, 7]. EFPI sensors are interferometric sensors, but they differ in number of essential optical fibers. EFPI sensors need only a single optical fiber because sensing and reference lights propagate in the same fiber. Therefore, installation of EFPI sensors into FRP is much easier than Michelson interferometric sensors. Since usual EFPI sensors have low temperature sensitivity, they are especially suited for monitoring in temperature-changeable conditions, such as those occurring during the curing process. It was reported that curing shrink and residual strain of FRP during cure could be monitored by using EFPI sensors [8–10].

FBG sensors have also become more popular in this decade. Since FBG is an optical grating written in a core of a fiber, these need no mechanical part. In addition, FBG sensors are independent upon optical loss and can be multiplexed easily because they use spectrum peak shifts for strain/temperature measurement. Therefore, FBG sensors are suitable for long-distance embedding in large composites. Several papers have addressed usage of FBG sensors during cure of FRP [12–14] and many researches on health monitoring by using FBG sensors were reported [15–17]. As for the application to damage detection, it was shown that FBG sensors could detect strain concentration caused by internal cracks

of FRP laminates as well as strain value [15]. B-OTDR is a sensing technique of strain/temperature distribution along usual optical fiber. Since B-OTDR fiber optic sensors have about 1m special resolution, they are preferred to integration into large composite structures. It was reported that B-OTDR fiber optic sensors were applied to health monitoring of a composites hull of a racing yacht [18].

We have applied EFPI and FBG strain monitoring systems to both cure and health monitoring of various kinds of FRP, such as autoclave-molded FRP, filament winding (FW) FRP, and RTM-molded textile FRP because their reinforcing configuration sometimes affects sensing function of embedded sensors [9, 10, 14]. However, there are a few studies on the application of fiber optic sensors to cure and health monitoring of braided composites. Braided composites are well suited for integration of fiber-shaped functional components because fibers can be integrated straightly into fabrics as warp. Therefore, functional performance of functional components can be maximized. Another advantage is that fiber optic sensors can be integrated automatically during braiding. From these advantages, it can be considered that braided composites are highly suitable for long continuous FRP parts including fiber optic sensors. In the present paper, EFPI and FBG sensors were embedded in flat-braided GFRP. Internal strain measurements of specimens were conducted during cure, in tensile test and in fatigue test. From the experimental results, self-monitoring function of braided FRP with built-in fiber optic sensors was discussed.

2. EXPERIMENTAL

2.1. Optical fiber sensors and sensing systems

Figure 1 illustrates constructions of EFPI and FBG sensors used in this study. Diameter of optical fibers for both sensors was 125 μm. Input and reflector fibers of EFPI sensors are adhered to a glass capillary tube of 310 μm diameter by polyimide adhesives. These two fibers are arranged axially with a air gap of 55 μm. The gauge length is defined as the distance between two adhered points. The reflected light is modulated by an EFPI and the spectrum has a cosine wave form when white light is input as shown in Fig. 1a. The gap length d can be calculated by the following equation from the reflected spectrum:

$$d = \frac{(N-1)}{2} \frac{\lambda_1 \lambda_N}{\lambda_N - \lambda_1}, \tag{1}$$

where, N is number of peaks and λ_i is a position of the ith peak. The axial strain ε_3 can be represented as

$$\varepsilon_3 = \frac{\Delta d - d_0 \alpha_S \Delta T}{L_G}, \tag{2}$$

where, L_G is a gauge length, d_0 is an initial cavity length, Δd is a variation of the gap length, α_S ($= 0.5 \times 10^{-6}$/°C) is a coefficient of thermal expansion (CTE) of

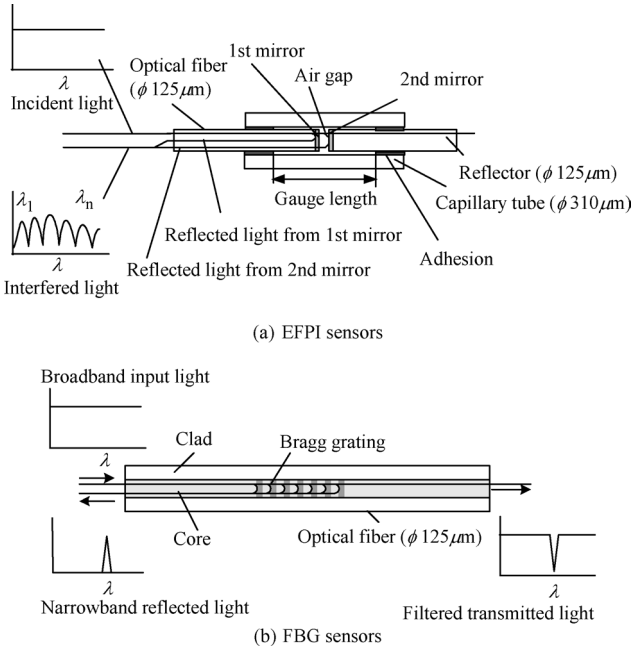

Figure 1. Constructions of EFPI and FBG sensors.

silica optical fibers and ΔT is a variation of temperature. Because the gauge length was about 4 mm and the initial length of air gap was about 55 μm, the EFPI sensors have low temperature sensitivity, which is about $0.0069 \times 10^{-6}/^{\circ}\mathrm{C}$.

On the other hand, FBG sensors have optical sensing parts (Bragg grating), which are periodical variations of refractive index of a fiber core. FBG sensors act as a narrow-band optical filter and a center wavelength of the reflected light indicates a strain-temperature coupled value. The strain output of FBG sensor was obtained from Bragg wavelength shift $\Delta\lambda$ and a temperature variation ΔT by the following equation [18]:

$$\frac{\Delta\lambda}{\lambda_0} = \left[1 - \frac{n_0^2}{2}\left\{p_{12} - \nu_s(p_{11} + p_{12})\right\}\right]\varepsilon_3 + \left(\alpha_s + \frac{1}{n_0}\frac{dn_0}{dT}\right)\Delta T, \tag{3}$$

where λ_0 is initial Bragg wavelength, p_{11} and p_{12} are Pockels constants, ν_s is Poisson ratio, n_0 is refractive index at $\Delta T = 0$. All values belong to the FBG sensor. In this paper, these sensor sensitivities to ε_3 and ΔT were already obtained before the strain measurement and the following equation was used for the calculation of strain.

$$\frac{\Delta\lambda}{\lambda_0} = 0.7368 \times \left(\varepsilon_3 - 0.5 \times 10^{-6} \times \Delta T\right) + 6.9032 \times 10^{-6} \times \Delta T. \tag{4}$$

Two types of sensing systems were used for the strain measurement as shown in Fig. 2. One is the OSA system which is composed of a super luminescence

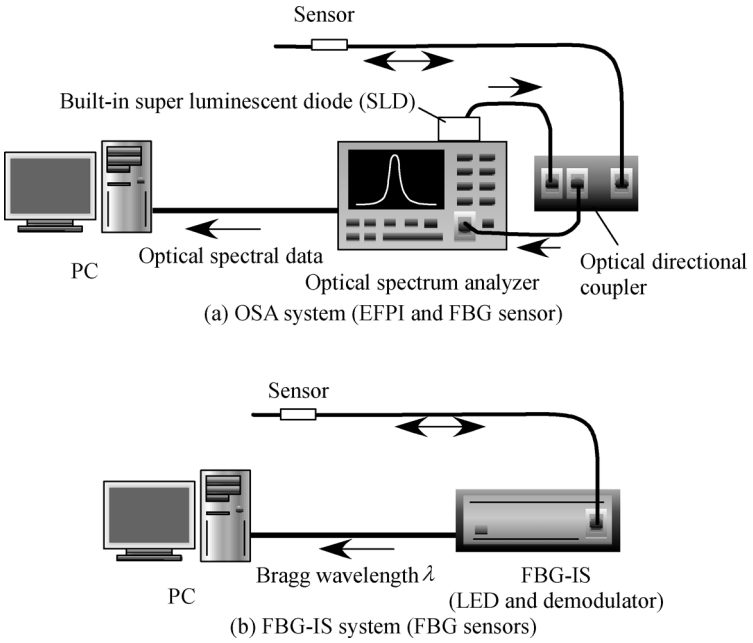

Figure 2. Sensing system for EFPI and FBG sensors.

diode (SLD), an optical spectrum analyzer (OSA; Anritsu MS9710) and an optical directional coupler. This system was used for acquisition of the reflected spectrum from the FBG and the EFPI sensors. The measured spectra were sent to PC and then strain was computed by using the equations (1)–(4). This system is especially useful for checking state of the sensors by observation of the reflected spectral shape. The OSA system is not suited for the measurement during the fatigue tests because the wavelength scanning takes about a few seconds. The wavelength resolution of the OSA system is 0.01 nm which was equivalent to 10×10^{-6} strain for the FBG sensors. The strain resolution of the EFPI sensors by using the OSA system was about 50×10^{-6} strain. Another system is the FBG-IS system (FBG-IS, Micron optics and NTT-AT). It reports only center wavelengths reflected from FBG sensors. Since this system has higher accuracy and speed (0.001 nm wavelength resolution and 50 Hz sampling frequency), it was applied to strain measurement during the fatigue tests.

2.2. Specimen

A glass fabric was braided by using glass fiber strands (ER11560-F165N, Nippon Electric Glass) and was cut to length of about 220 mm. Then, fiber optic sensors were installed straightly in a braided fabric as illustrated in Fig. 3. Figure 4 shows a schematic view of a mold. A flat braided fabric and steel spacers were sandwiched by Teflon sheets and steel base plates. The Teflon plates were placed with a space of 23 mm in parallel and sealants were used as a dam. An optical fiber was drawn

from surface of the braded fabric and set through a U-groove of the upper steel plate to prevent optical power loss by local bending at the egress point. After setting the fabric to the mold, the fabric was impregnated with vinylester resin (Ripoxy R-802, Showa Highpolymer), which was defoamed in a vacuum chamber for 10 min. The curing conditions were: heating up to 80°C for 1 h, holding for 5 h and natural cooling. Strain and temperature were measured during the molding process by using an embedded fiber optic sensor and a thermocouple. The molded FRP had a nonlinear stress–strain behavior, the initial stiffness from 12.6 to 14.6 MPa and the volume fraction from 34 to 40%. After the molding, specimens were cut and aluminum tabs were adhered to them. In mechanical loading tests, surface strain was also measured by attached strain gauges.

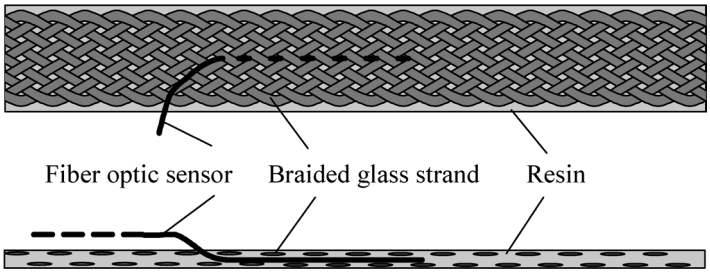

Figure 3. Embedding configuration of fiber optic sensors into braided FRP.

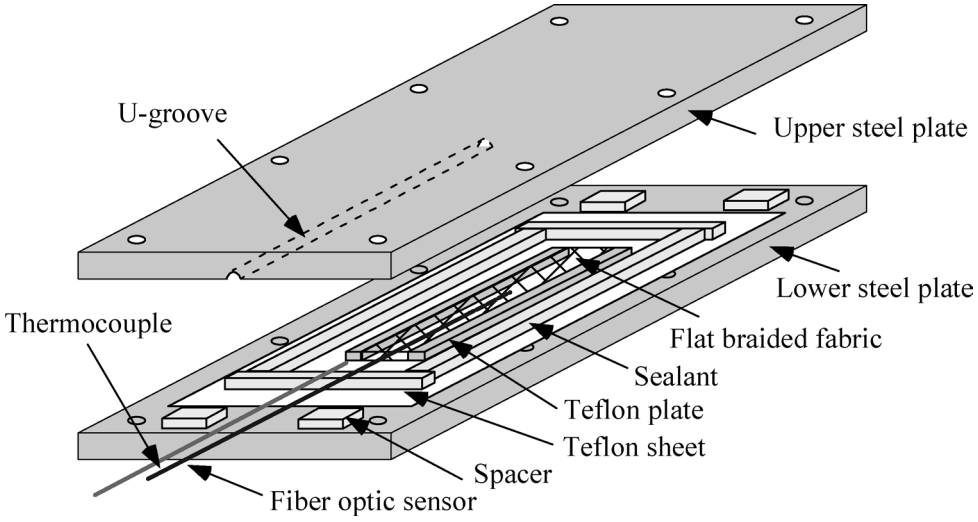

Figure 4. Schematic view of a mold.

3. EXPERIMENTAL RESULTS AND DISCUSSION

3.1. Internal strain measurement during cure

Because the optical fibers were drawn from the surface of the fabric, it could be considered that the optical power loss became lager than when the optical fibers were drawn from the end. In order to confirm the molding setup was valid for measurement of the strain monitoring during cure, the optical loss that occurred during the cure process was measured by using an optical power meter. From the results of the optical loss test, it was found that the maximum loss was 0.7 dB, which was so small that it did not affect reliability of embedded fiber optic sensors.

Internal strain profiles measured by FBG and EFPI sensors using the OSA system during curing process are plotted against time with temperature in Fig. 5. Both sensors detected thermal strain at the heating and the cooling stages, but could not detect curing shrink. Therefore, it was found that thermal strain governed residual curing strain for the FRP used in this study. At the heating stage, the detected strain by the FBG sensor was different from that using the EFPI sensor. Because the effective stiffness of the EFPI sensors was different from that of the FBG sensors due to the difference of the sensor diameters, it can be considered that the strain transmitted from low-stiffness curing resin to these sensors during cure showed different values at the heating stage. During cooling, both sensors detected almost the same compressive strain as each other. Therefore, it can be concluded that both

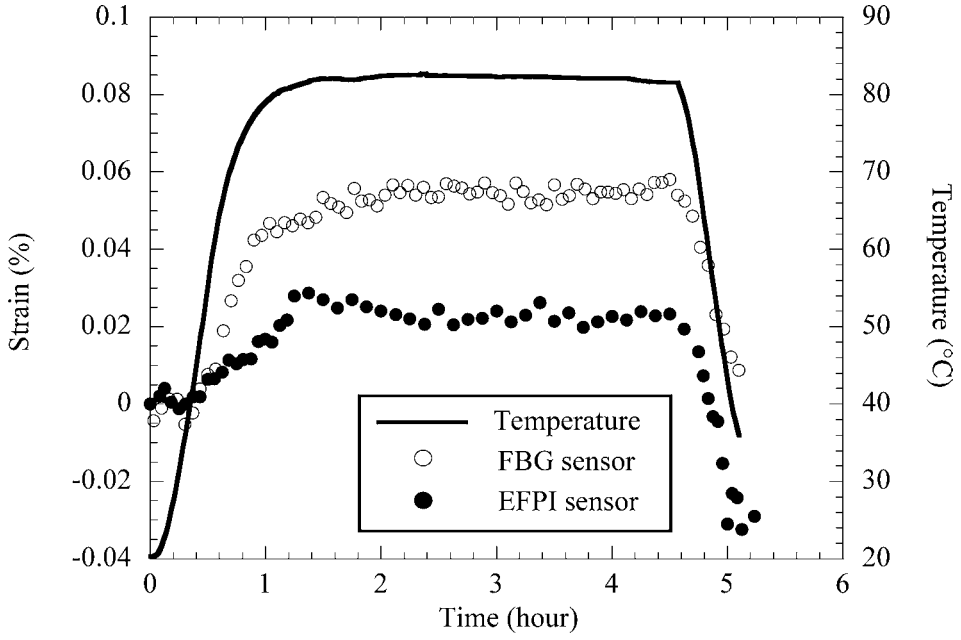

Figure 5. Strain from FBG sensor and EFPI sensor, and temperature *vs.* time in curing process (OSA system).

sensors embedded in braided FRP can be used for monitoring of residual strain during cure.

3.2. Internal strain measurement in tensile tests

The dimensions of the specimens were 23 × 190 × 1.1 mm ($W \times L \times T$). Tensile tests were conducted by using a universal testing machine (Instron Fast Track 8801, Instron, Inc.) under displacement control at speed of 0.02 mm/min. Figure 6 shows stress–strain curves from an embedded EFPI sensor and attached foil strain gauges. The experimental results showed that embedded EFPI sensors in braided FRP could measure internal strain over 2.0% strain although the good agreement between both sensor outputs was held within 0.8% strain. From the observation by optical microscope, it was found that the error of strain by the EFPI sensor in large strain range was produced by break of the capillary tube. However, the observation of spectrum from the EFPI sensor showed good interference, which means that there was no discrepancy of optical axis, until the break. Therefore, it was found that large axial strain affects precision of strain and the break of the capillary tube could not be detected.

Figure 7 shows stress–strain curves from an embedded FBG sensor and attached foil strain gauges in tensile tests. It was found that FBG sensors could measure internal strain correctly up to about 0.8% strain. At about 0.8% strain, the output of the FBG sensor jumped discontinuously and the difference of the curves between the FBG sensor and the strain gauges increased. To investigate the behavior of FBG sensors, an FBG spectrum, which gives us information of strain distribution applied to the sensing part, was observed in the tensile tests. Figure 8 shows the spectra from the embedded FBG sensor at various strains. Since the shape of the spectrum changed gradually from single peak to double peaks with increasing strain, it appeared that local strain distribution around the FBG sensor affects the reflected

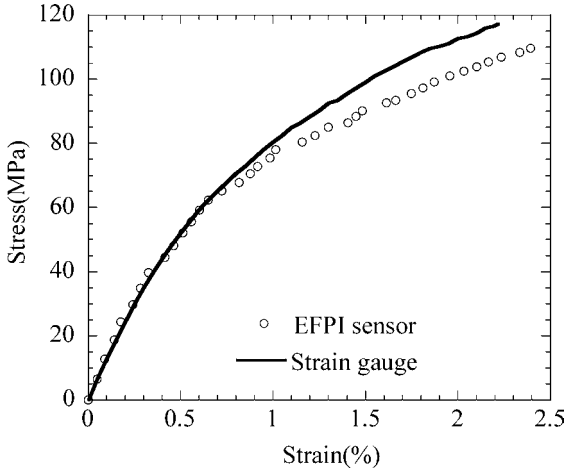

Figure 6. Stress–strain curves from FBG sensor and foil strain gauge in tensile tests (OSA system).

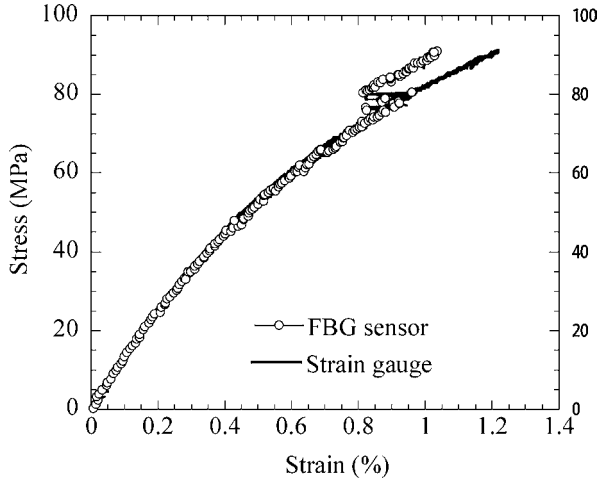

Figure 7. Stress–strain curves from FBG sensor and foil strain gauge in tensile tests (OSA system).

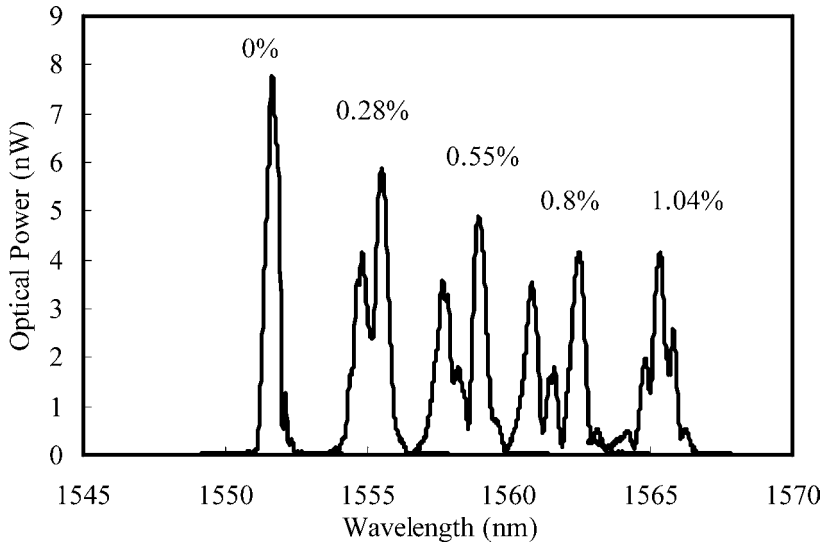

Figure 8. Spectra from FBG sensor in tensile tests (OSA system).

spectrum. However, the effect of changes in the spectral shape on the precision of strain sensing was very minor at about 0.8% strain as shown in Fig. 7. The sensor was not broken because the change in the optical power reflected from the FBG sensor was small. Therefore, it can be considered that the sudden change in the spectral shape resulted from the redistribution of strain caused by the initiation of damage near the sensor at the 0.8% strain.

3.3. Internal strain measurement in fatigue tests

Fatigue tests were conducted under load control by using the same testing machine used in the tensile tests. The dimensions of the specimens were 23 × 200 × 1.3 mm

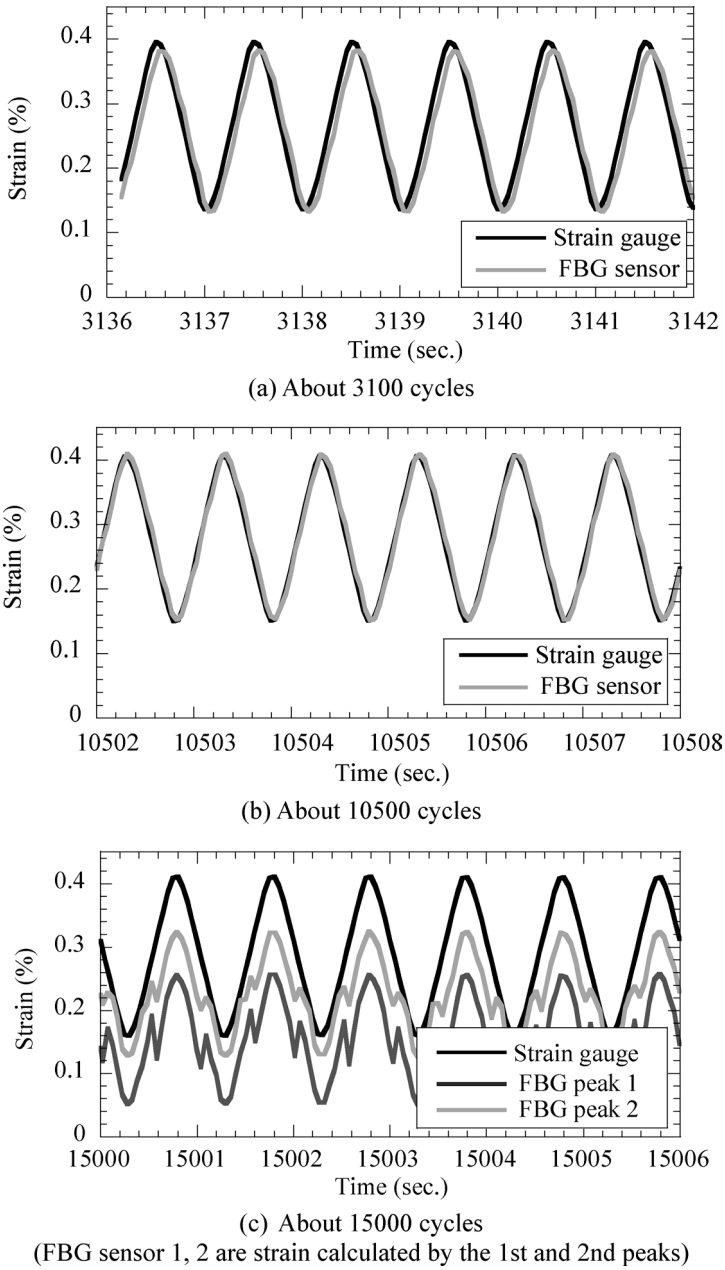

Figure 9. Time–strain curves obtained by an embedded FBG sensor and an attached strain gauge in fatigue tests ((a) 3100, (b) 10 500 and (c) 15 000 cycle).

($W \times L \times T$). The fatigue frequency was 1 Hz and the peak-to-peak amplitude of the sinusoidal load was 0.3 to 1.1 kN (9.94 MPa to 36.5 MPa stress). Time–strain curves obtained by an embedded FBG sensor and attached strain gauges at about 3100, 10 500 and 15 000 cycles are shown in Fig. 9a–c, respectively. These figures show that output of the FBG sensor agreed well with the strain gauge before about 10 500 cycles. At about 15 000 cycles, behavior of the curve obtained from the FBG sensor became different from the strain gauges. In Fig. 9c, two strain curves (FBG peaks 1 and 2) measured from the FBG sensor were shown because the number of spectral peaks increased. The graph shows the FBG sensor output jump to the other peaks when loading and unloading. Figure 10 shows a photograph of specimens after 15 000 cycles. In the photograph, many matrix cracks along the reinforcements can be observed as whitened region. Therefore, it can be considered that the reflected single-peak spectrum became twin peaks by the strain concentration caused by the cracks of braided FRP. To investigate the detail effect of the cracks to the FBG sensors, the reflected spectra were observed. Figures 11a–c show the reflected spectra at 10 000, 14 100 and 14 200 cycles when 0.4% strain was applied. The figure shows the spectrum has almost same shape until 14 100 cycles, but it dramatically changed into three peaks from 14 100 to 14 200 cycles. Since rapid increase of matrix cracks was observed from 14 100 to 14 200 cycles, it can be concluded that the matrix cracks strongly affected the spectral shape. These experimental results tell us that embedded FBG sensors in braided FRP have the capability of a self-monitoring function for fatigue damage.

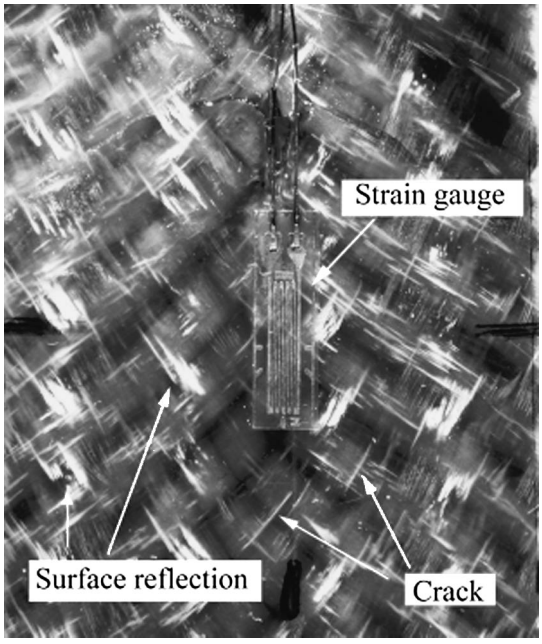

Figure 10. Photograph of specimen after fatigue crack initiation in fatigue tests.

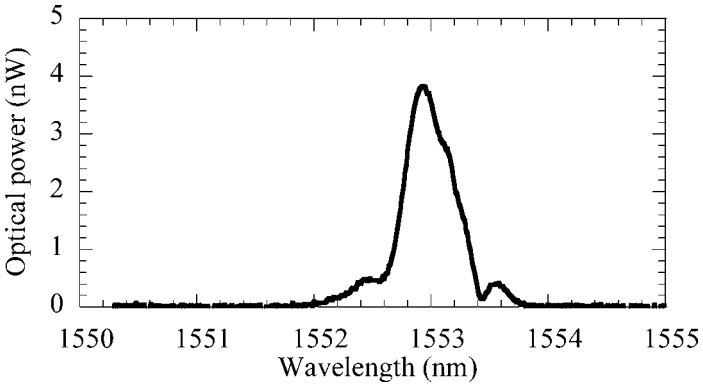

(a)

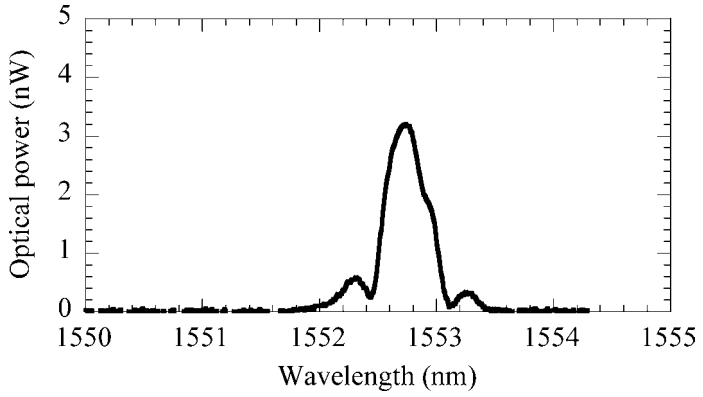

(b)

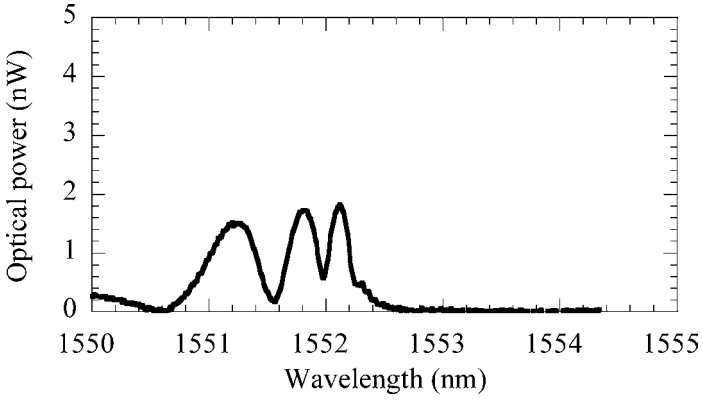

(c)

Figure 11. Reflected spectra from an embedded FBG sensor at 0.4% strain measured by strain gauge in fatigue tests ((a) 10 000, (b) 14 100 and (c) 14 200 cycle).

4. CONCLUSIONS

Strain monitoring of braided GFRP composites during cure, tensile tests and fatigue tests was conducted by using embedded FBG and EFPI sensors. From the experimental results of cure monitoring, it was found that both sensors can be used only for monitoring of thermal residual strain during cooling process. From the results of tensile tests, it was found that both sensors could measure strain correctly until damage initiation of braided FRP, which occurs at 0.8% strain, while outputs of the sensors showed error in large strain. In addition, it appeared that the FBG sensors could monitor damage of FRP near the sensor by observing the reflected spectral shape during tensile tests and fatigue tests.

REFERENCES

1. T. Fukuda and T. Kosaka, Cure and health monitoring, in: *Encyclopedia of Smart Materials*, M. Schwartz (Ed.), John Wiley, New York, ISBN: 0-471-17780-6 (2002) (in print).
2. G. R. Powell, P. A. Crosby, D. N. Waters, C. M. France, R. C. Spooncer and G. F. Fernando, In-situ cure monitoring using optical fibre sensors — a comparative study, *Smart Mater. Struct.* **7** (4), 557–568 (1998).
3. C. Doyle, A. Martin, T. Liu, M. Wu, S. Hayes, P. A. Crosby, G. R. Powell, D. Brooks and G. F. Fernando, *In-situ* process and condition monitoring of advanced fibre-reinforced composite materials using optical fibre sensors, *Smart Mater. Struct.* **7** (2), 145–158 (1998).
4. H. J. Paik and N. H. Sung, Fiber-optic intrinsic fluorescence for *in-situ* cure monitoring of amine cured epoxy and composites, *Polym. Engng Sci.* **34** (12), 1025–1032 (1994).
5. Y. M. Liu, C. Ganesh, J. P. H. Steele and J. E. Jones, Fiber-optic sensor development for real-time *in-situ* epoxy cure monitoring, *J. Compos. Mater.* **31** (1), 87–102 (1997).
6. H. Tsuda, S. Takeda, J. Takahashi and K. Urabe, Response of Michelson interferometric fiber-optic sensors to impact loading, *J. Mater. Sci. Letters* **19** (1), 1 (2000).
7. T. Fukuda, K. Osaka and S. Kitade, Measurement of strain and detection of cracking in graphite-epoxy composites with embedded optical fibers, *J. Soc. Mat. Sci., Japan* **42** (474), 269–275 (1993).
8. A. L. Kalamkarov, S. B. Fitzgerald and D. O. MacDonald, The use of Fabry–Perot fiber-optic sensors to monitor residual strains during pultrusion of FRP composites, *Composites: Part B* **30**, 167–175 (1999).
9. K. Osaka, T. Kosaka, Y. Asano and T. Fukuda, Measurement of internal strains in FRP laminate with EFPI optical fiber sensor during autoclave molding; measurement in off-axis directions, in: *Proc. the 2nd Asian-Australasian Conf. on Composite Materials (ACCM-2000)*, Kyongju, Korea, pp. 1117–1122 (2000).
10. T. Kosaka, K. Osaka, M. Sando and T. Fukuda, Curing strain monitoring of FRP FW pipe with EFPI fiber-optic sensors, in: *Materials Science Research International — Special Technical Publication,* Vol. 2, pp. 100–104 (2001).
11. V. M. Murukeshan, P. Y. Chan, L. S. Ong and L. K. Seah, Cure monitoring of smart composites using fiber Bragg grating based embedded sensors, *Sensors and Actuators: A Phys.* **79** (2), 153–161 (2000).
12. P. A. Crosby, C. Doyle, C. Tuck, M. Singh and G. F. Fernando, Multi-functional fiber-optic sensors for cure and temperature monitoring, in: *Proc. SPIE*, Vol. 3670, pp. 144–152 (1999).
13. T. Kosaka, K. Osaka, Y. Asano and T. Fukuda, Cure and health monitoring of RTM molded FRP by using optical fiber strain sensors, in: *Extended Abstracts of 5th International Conference*

on Durability Analysis of Composite Systems (DURACOSYS 2001), Tokyo, Japan, pp. 138–142 (2001).
14. Y. Okabe, S. Yashiro, T. Kosaka and N. Takeda, Detection of transverse cracks in CFRP composites using embedded fiber Bragg grating sensors, *Smart Mater. Struct.* **9** (6), 832–838 (2000).
15. Y. J. Rao, D. A. Jackson, L. Zhang and I. Bennion, Strain sensing of modern composite materials with a spatial/wavelength multiplexed fibre grating network, *Opt. Lett.* **21**, 683–685 (1996).
16. X. Tao, L. Tang, W. C. Du and C. L. Choy, Internal strain measurement by fiber Bragg grating sensors in textile composites, *Compos. Sci. Technol.* **60** (5), 657–669 (2000).
17. H. Murakami, K. Kageyama, I. Kimpara, A. Shimada and H. Naruse, Strain monitoring of IACC yachts using fiber-optic distributed sensors, in: *Proc. 9th US-Japan Conf. Compos. Mater.*, Mishima, Japan, p. 159 (2000).
18. Y. J. Rao, Recent progress in applications of in-fibre Bragg grating sensors, *Opt. Lasers Eng.* **31** (4), 297–324 (1999).